The 2021 World Congress on
Advances in Structural Engineering and Mechanics (ASEM21)
GECE, Seoul, Korea, August 23-26, 2021

Keynote Paper

Performance-based seismic assessment of slab-column frames

Yan Zhou[1] and *Mary Beth D. Hueste[2]

[1] *School of Civil Engineering, Changsha University of Science and Technology, Changsha, Hunan, China*
[1] *yan.zhou@csust.edu.cn*

[2] *Zachry Department of Civil and Environmental Engineering, Texas A&M University, College Station, Texas, USA*
[2] *mhueste@tamu.edu*

ABSTRACT

The two-way shear response of slab-column connections has been evaluated by a significant number of experiments. This paper summarizes an updated database of slab-column connection tests that have been documented in the literature using consistent criteria for selecting key response parameters including the limiting lateral drift capacity and gravity shear ratio. The collected test results include interior reinforced concrete (RC) and post-tensioned (PT) concrete slab-column connections without shear reinforcement under combined lateral and gravity shear demands. This database has been used to develop recommended modeling parameters to define the force-deformation backbone relationships for slab-column connection components. The proposed modeling parameters are derived considering a detailed review of the backbone response in the experimental database. Recommendations for updates to the current modeling parameters found in ASCE 41-17 are provided. A nonlinear model monitoring column drift to capture punching shear failure for slab-column connections was developed to model the lateral load response of slab-column frame members. The proposed nonlinear modeling parameters are validated from experiments reported in the literature using the developed punching shear model. Strength and stiffness in modeling and analysis of slab-column frames are also discussed.

1. INTRODUCTION

Past earthquake damage and experimental evidence have shown that slab-column (SC) frames are vulnerable to brittle punching shear failures under lateral load demands. The *ASCE 41-17: Seismic Evaluation and Retrofit of Existing Buildings* (ASCE 2017) standard provides guidance for evaluating the seismic performance of existing buildings

---

[1] Assistant Professor
[2] Professor

using both linear and nonlinear methods of analysis.

ASCE 41-17 defines nonlinear modeling parameters for the structural component force versus deformation (backbone) relations for nonlinear analysis. Fig. 1 shows the definition of parameters ***a***, ***b***, ***c***, ***d***, and ***e*** for reinforced concrete (RC) and post-tensioned (PT) components. The resistance ratio on the vertical axis $Q/Q_y = 1.0$ represents yielding. Parameters ***a***, ***b***, ***d***, and ***e*** are plastic deformations, and are taken as the plastic drift or rotation corresponding to the significant loss of lateral force carrying capacity (***a*** and ***d***) and the loss of gravity load carrying capacity (***b*** and ***e***), respectively. Parameter ***c*** is taken as the residual force capacity that corresponds to 20% of the peak lateral loading.

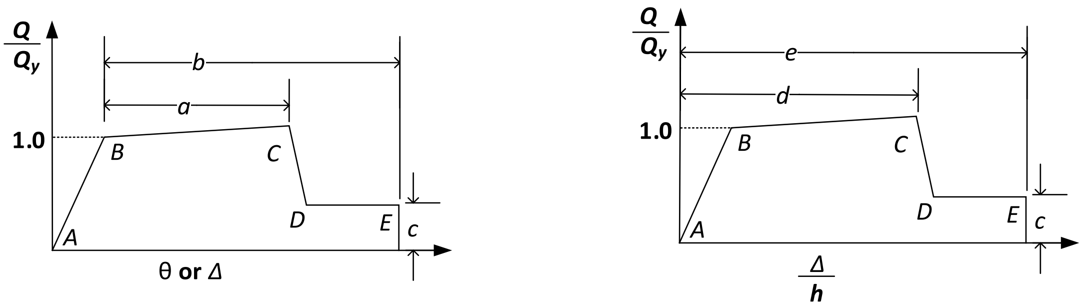

(a) Deformation (b) Deformation ratio

Fig. 1. Generalized force-deformation relation (adapted from ASCE 41-17).

The current study reviews the lateral deformation capacity of RC and PT SC connections and the corresponding ASCE 41-17 modeling parameters for nonlinear analysis. An updated database of RC and PT SC connection tests for combined shear and unbalanced moment has been compiled and includes tests not considered in the development of the current ASCE 41 parameters ***a*** and ***b*** (Zhou and Hueste 2017). The database is reviewed using consistent criteria to select key response parameters from the experimental results including the drift at yield, the drift where significant strength degradation begins, and the drift corresponding to the loss of seismic-force-resisting capacity. Further, a nonlinear model, including the occurrence of punching shear failures, is developed for lateral load analysis and implemented in OpenSees (Open System for Earthquake Engineering Simulation) (McKenna et al. 2000). The proposed model directly links the punching shear failure to the column drift of SC connections. The proposed model is validated using SC connection tests in the literature.

2. PROPOSED NONLINEAR MODELING PARAMETERS

Fig. 2 to Fig. 5 depict the proposed modeling parameters ***d*** and ***e*** for a given gravity shear ratio (*VR*) determined for the updated SC connection database. *VR* is determined as $V_g/\phi V_c$, where V_g is the reported direct shear force transferred at the critical shear perimeter of the SC connection, V_c is the two-way concrete shear strength calculated in accordance with ACI 318-19 (ACI Committee 318 2019) Section 22.6.5 using the reported measured material properties and specimen geometry, and ϕ=1.0. The red lines provide the ASCE 41-17 values based on modeling parameters ***a*** and ***b*** plus the assumed yield rotation (0.010 radians for RC and 0.015 radians for PT SC connections, respectively) assumed by Elwood et al. (2007). For simplicity, it is proposed to estimate modeling parameters using a bilinear approximation of the mean for RC and PT specimens with *continuous* bottom reinforcement, given by the green lines in Fig. 2 to Fig. 5.

Limited data are available for RC and PT SC connection specimens with *discontinuous* bottom bars, as shown in Fig. 3(b) and Fig. 4(b). SC frames constructed without continuity reinforcement are more likely to undergo loss of gravity load resistance after a punching shear failure, leading to structural collapse. The proposed parameter ***d*** for SC connections without continuity reinforcement is set to reach the approximate lower bound *DR*. Due to limited data, the proposed parameter ***e*** values for SC connections without continuity reinforcement are taken to be equal to the proposed values for parameter ***d***.

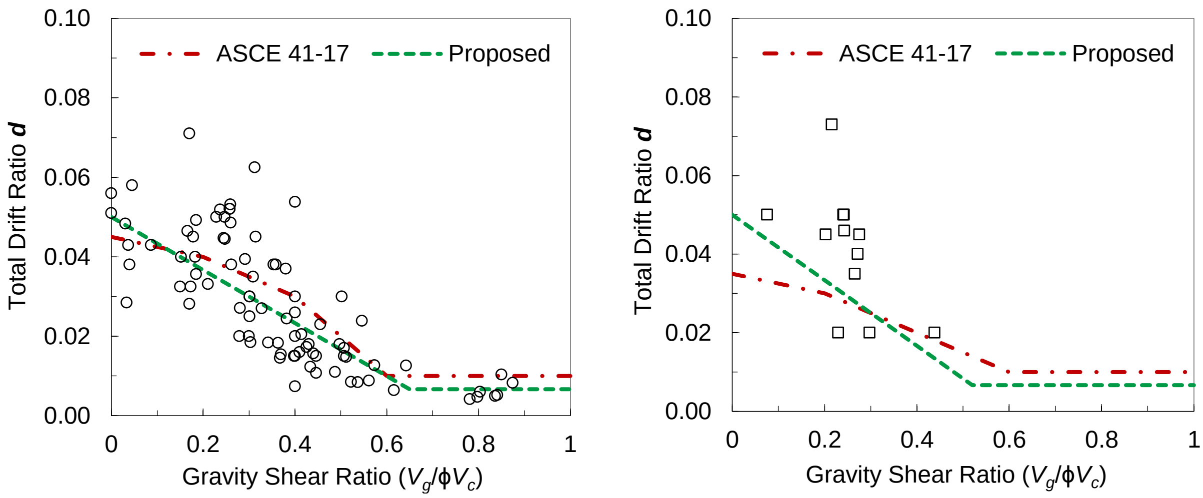

(a) with continuity reinforcement (b) without continuity reinforcement

Fig. 2. Proposed ***d*** for RC SC connections.

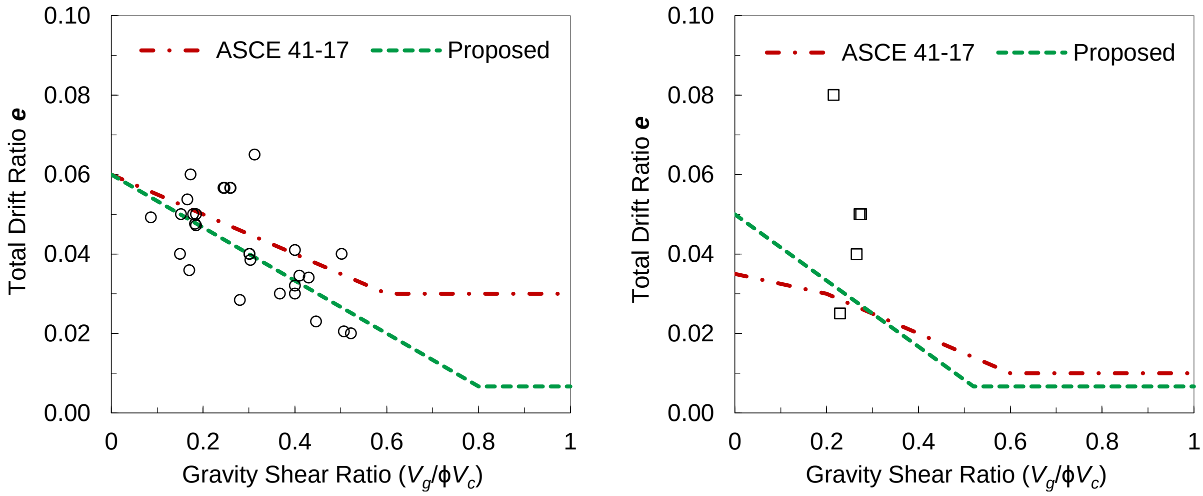

(a) with continuity reinforcement (b) without continuity reinforcement

Fig. 3. Proposed ***e*** values for RC SC connections.

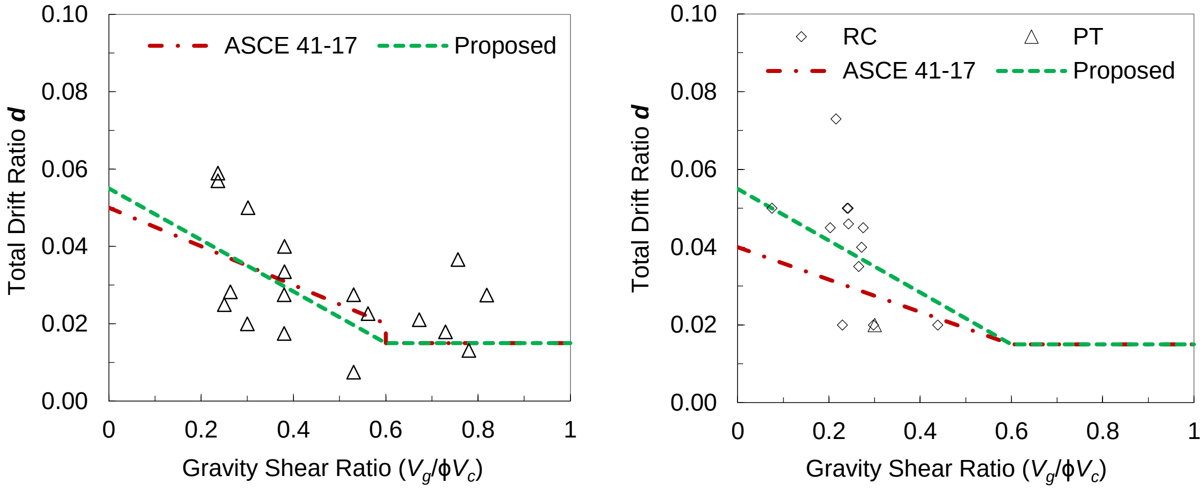

(a) with continuity reinforcement (b) without continuity reinforcement

Fig. 4. Proposed ***d*** for PT SC connections.

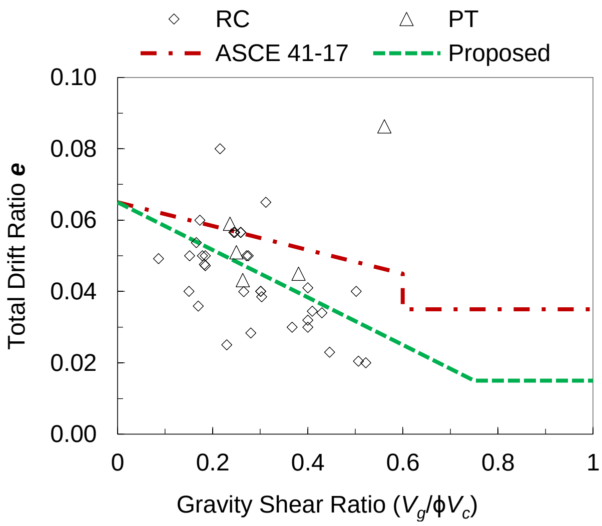

Fig. 5. Proposed ***e*** for PT SC connections with continuity reinforcement.

3. Model to Capture Punching Shear Failure

A model to capture punching shear failure was developed that can use the limiting drift value determined from the experimental database. The OpenSees program was considered for implementation as it provides an open platform and has become relatively popular among users of nonlinear analysis tools for earthquake engineering.

The nonlinear fiber column element in OpenSees is used to model the columns of the SC frames. The slab is modeled using an elastic beam element based on an effective slab width, with the plastic behavior of the slab assumed to be concentrated at the slab ends as shown in Fig. 6. In the proposed limit state model, a punching shear failure is detected when the column *DR* exceeds a given *DR* limit. This concept is more directly linked to the experimental data. This study considered both the current ASCE 41-17 modeling parameters and the proposed modeling parameters.

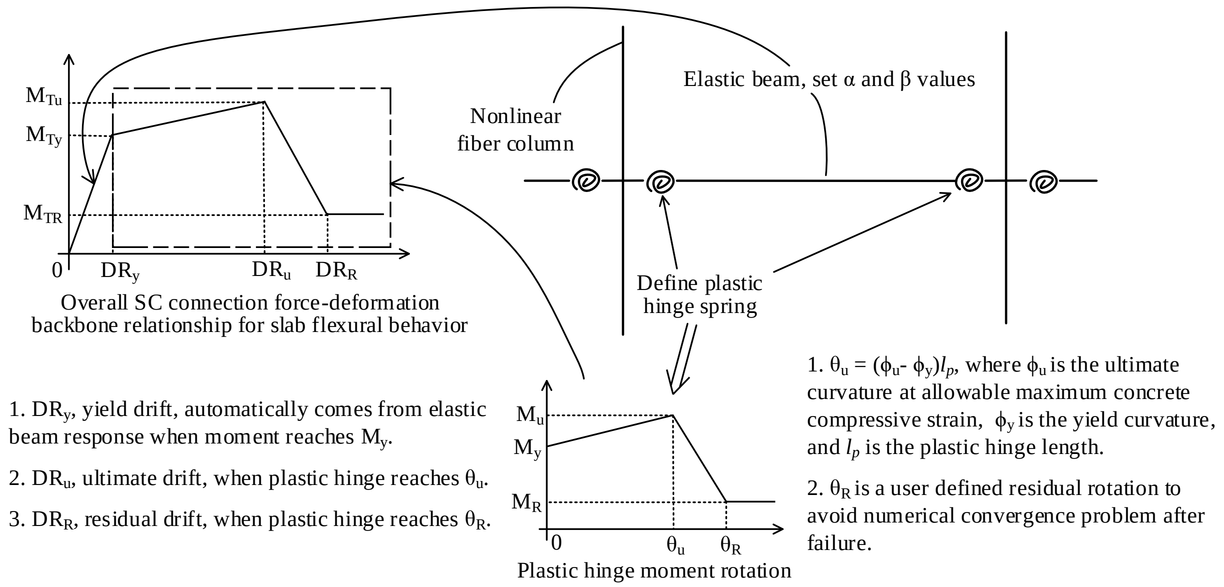

Fig. 6. Model for SC frames.

4. Verification of Nonlinear Model with Experimental Results

Published results for RC and PT SC connection specimens were used in the verification of the developed nonlinear model. To avoid uncertainties and improve modeling accuracy, SC connection tests in the literature with appropriate reported details in test setup, lateral displacement routine, specimen design (i.e., column and slab reinforcement layout details), and material properties were selected. OpenSees models were developed to represent the boundary conditions of these test configurations. In the OpenSees analysis, the effective slab width factors (αβ) are adjusted to best replicate the experimental backbone response, where α is defined as the effective slab width and β is defined as effective stiffness factor for cracked section of a slab.

4.1 Verification of Punching Shear Model

The developed limit state punching shear model was tested in OpenSees using SC connection specimens from the literature (Zhou 2019). An interior SC connection specimen, 7L tested by Robertson (1990), was included in the verification. As shown in Fig. 7, the developed punching shear model correctly detects the *failure* at *DR* limit= 1.5 percent. In addition, the residual moment capacity was reduced to a user-defined amount (M_R = 0.40M_u) to best replicate the experimental backbone response. The verification results show that the proposed limit state punching shear model can capture the overall hysteretic response for tested SC connections.

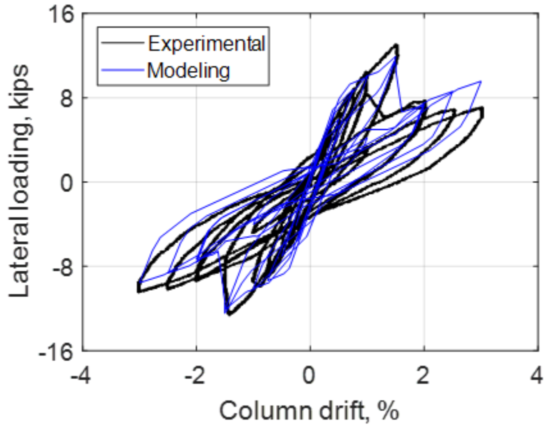

VR = 0.37, *DR* limit = 1.5% (1 kip=4.45 kN)
Specimen 7L (*Robertson 1990*).
Fig. 7. Limit state punching shear model results.

4.2 Reinforced Concrete Slab-Column Connections

A SC connection specimen, 8I (Robertson 1990), was among the RC SC specimens selected for verification. Modeling results, shown in Fig. 8, provide a comparison of the overall behavior SC connection behavior. The black lines represent the experimental backbone response, while the blue lines correspond to the modeled backbone response using the proposed approach and proposed modeling parameter ***d*** (M1). The purple lines show the modeled backbone response using the ASCE 41 approach with ASCE 41 modeling parameters ***a*** and ***b*** (M2). For this comparison, the αβ value for M1 is manually adjusted to replicate the initial stiffness of the experimental backbone response. However, the αβ value for M2 is calculated based on definitions in ASCE 41-17.

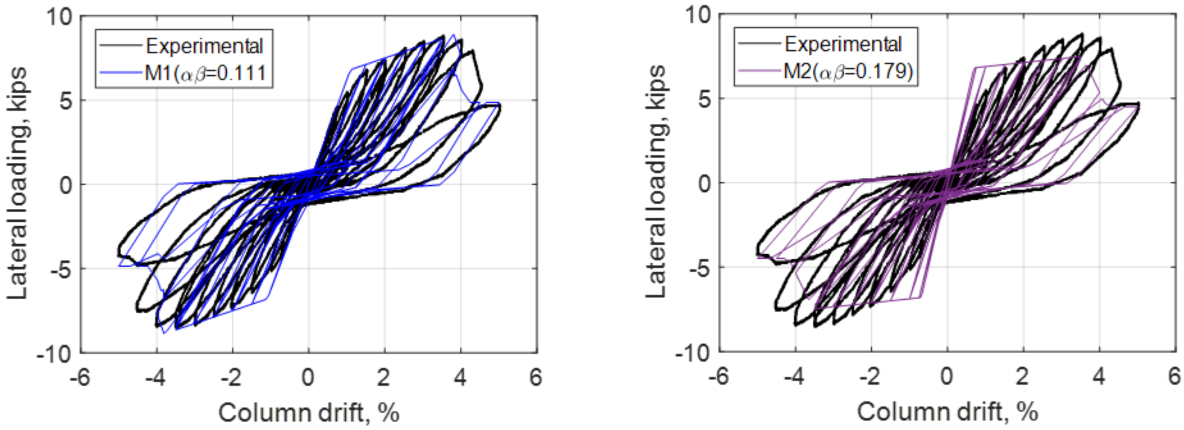

(a) Proposed method (1 kip=4.45 kN) (b) ASCE 41 method (1 kip=4.45 kN)

Fig. 8. Model results for specimen 8I tested by Robertson (1990).

Slab effective stiffness. Fig. 8(b) indicates that the αβ value calculated from the ASCE 41 recommendations for specimen 8I slightly overestimate the initial stiffness.

Maximum lateral strength. The flexural strength of slab column strip was used in the modeling analysis for both the proposed and ASCE 41 methods. M1 (proposed) indicates a lateral strength slightly greater than the experimental values for yielding, and M2 (ASCE 41) shows a lateral strength slightly greater than the experimental values for yielding and slightly less than the experimental values for the peak.

Column drift at failure. The ratio of modeling *DR* at failure to experimental *DR* at failure for M1 (proposed) and M2 (ASCE 41) are 0.84 and 0.78, respectively. Both predictions are lower than the experimental result.

Slab plastic hinge rotation at failure. M1 (proposed) is monitoring the column drift to predict failure, whereas M2 (ASCE 41) is defining the slab plastic hinge rotation to predict failure. The plastic rotation value for M1 is the slab rotation when a column *DR* limit is detected. The plastic rotation value for M2 is the approximate rotation values provided in the ASCE 41-17 Table 10-15 as a function of *VR*. The plastic rotations for M1 are +/-0.026, and the plastic rotations for M2 are +/-0.030.

4.3 Post-Tensioned Slab-Column Connections

One PT SC connection specimen (PI-B30) tested by Han et al. (2006) is selected for model verification. Modeling results are shown in Fig. 9 for comparison of the overall behavior of the SC connections.

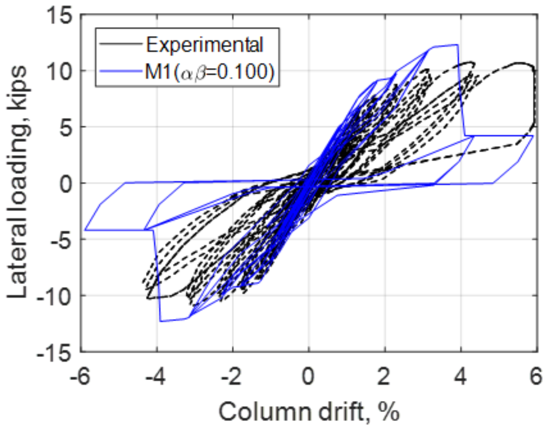

(a) Proposed method

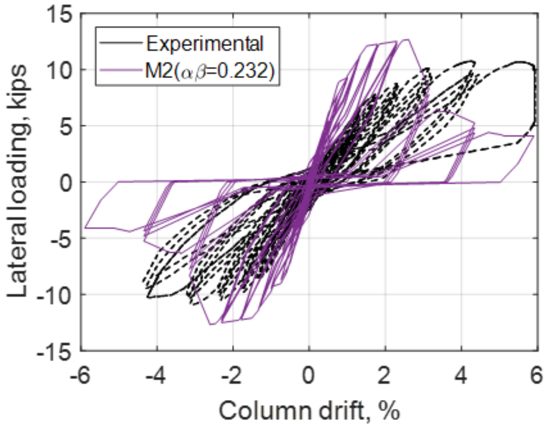

(b) ASCE 41 method

Fig. 9. Model results for specimen PI-B30 tested by Han et al. (2006).

Slab effective stiffness. Fig. 9(b) indicate that the αβ value calculated from the ASCE 41 recommendations for specimen PI-B30 overestimates the initial stiffness.

Maximum lateral strength. M1 (proposed) indicates a lateral strength slightly greater than the experimental values, and M2 (ASCE 41) shows a lateral strength greater than the experimental values.

Column drift at failure. The ratio of the model *DR* at failure to experimental *DR* at failure for M1 (proposed) and M2 (ASCE 41) are 0.66 and 0.44, respectively. Both predictions are lower than the experimental result.

Slab plastic hinge rotation at failure. The plastic rotations for M1 are +0.006/-0.033, and the plastic rotations for M2 are +/-0.023.

6. SUMMARY AND CONCLUSIONS

Based on the updated database for RC interior SC connections with and without continuous bottom bars under combined lateral and gravity shear loading, nonlinear modeling parameters ***d*** and ***e*** are developed to estimate the lateral force-deformation backbone relations, as follows.

- For RC and PT SC connections with continuous bottom bars, the proposed ***d*** and ***e*** values are based on the approximate mean values of the combined dataset.
- For RC and PT SC connections with discontinuous bottom bars, the test data are very limited. Therefore, the proposed ***d*** and ***e*** values are taken to be equal.
- The proposed punching shear model is able to represent the intended cyclic behavior for SC connections.

Sample modeling validations based on experimental data have been provided. Additional validation was conducted as part of this study (Zhou 2019). Based on the observation of the modeling validations, conclusions are drawn as follows.

- For the modeling stiffness, $\alpha\beta$ values based on the ASCE 41 recommendations are likely to overestimate the initial stiffness for isolated SC connection tests.
- For modeling strength, the flexural strength over the slab column strip is able to provide a reasonable estimate of the experimental results.
- For the drift ratios (*DR*s) at failure, the proposed method predicts drifts less than the experimental values. However, the ASCE 41 method predicts drifts significantly less than the experimental *DR*s.
- For the slab end plastic rotation at failure, it is observed that to reach a defined column *DR*, the plastic hinge rotation reaches a value larger than that corresponding to the defined column *DR* minus the yield rotation.

REFERENCES

ACI Committee 318 (2019). “Building code requirements for structural concrete and commentary.” *ACI 318-19*, American Concrete Institute (ACI), Farmington Hills, MI.

ASCE (2017). “Seismic evaluation and retrofit of existing buildings.” *ASCE/SEI 41-17*, American Society of Civil Engineers (ASCE), Reston, VA.

Elwood KJ, Matamoros AB, Wallace JW, Lehman DE, Heintz JA, Mitchell AD, Moore MA, Valley MT, Lowes LN, Comartin CD, Moehle JP. Update to ASCE/SEI 41 concrete provisions. *Earthquake Spectra*, 2007; **23**(3): 493-523.

Han, S. W., Kee, S., Kang, T. H., Ha, S., Wallace, J. W., and Lee, L. (2006). “Cyclic behaviour of interior post-tensioned flat plate connections.” *Magazine of Concrete Research*, **58**(10), 699-712.

McKenna, F., Fenves, G. L. and Scott, M. H. (2000), “Open system for earthquake engineering simulation,” *Pacific Earthquake Engineering Research (PEER) Center*, University of California, Berkeley, CA.

Robertson, I.N. (1990). “Seismic response of connections in indeterminate flat-slab subassemblies.” *Ph.D. Dissertation*, Rice Univ., Houston, TX.

Zhou, Y. and Hueste, M.D. (2017), "Review of Test Data for Interior Slab-Column Connections with Moment Transfer," *ACI Special Publication SP-315 and fib Bulletin 81 – ACI-fib International Symposium on Punching Shear of Structural Concrete Slabs: Honoring Neil M. Hawkins*, American Concrete Institute (ACI) and fib (International Federation for Structural Concrete), SP-**315**-08, 141-166.

Zhou, Y. (2019). "Seismic Performance Assessment and Nonlinear Modeling Parameters for Slab Column Connections." *Ph.D. Dissertation*, Texas A&M University, College Station, TX.